



Integrated Full-Bridge-Forward DC–DC Converter for a Residential Micro Grid Application

P.Simhachalam

Asst. Professor, Dept. of EEE, Indo American Institutions Technical Campus, Visakhapatnam, Andhrapradesh, India

ABSTRACT: This paper proposes a novel integrated converter topology for interfacing between the energy storage system and the dc bus for a residential micro grid application. The proposed integrated full-bridge-forward dc–dc converter presents the following features: low number of active devices compared to the converters usually applied to similar applications, low input and output current ripple, high voltage ratio, bidirectional power flow, and galvanic isolation. A double-ended forward converter with particularities such as no extra transformer demagnetizing circuit is originated from the integration process. This converter is approached in detail in this paper, including three different clamping circuits which are analyzed and compared. The structure, principle of operation, analysis, transformer design methodology, comparison with the dual active bridge converter, and experimental results of the proposed topology are presented.

KEYWORDS: DC bus interconnection, dc–dc converter, energy storage system, micro grid, power converter integration.

I. INTRODUCTION

Electrical energy consumption has been increasing in recent years, and this fact has been essential to the in-crease of electric power generation. Distributed generation (DG) technologies have been gaining interest due to some benefits such as high reliability, high power quality, and modularity, efficiency, reduced or absent emissions, security, and load management [1], [2]. However, the uncontrolled use of individual DG units can cause various problems thereby compromising their benefits [3], [4]. Difficulties in connecting these units directly to the bulky ac system due to their variable and intermittent power generation, voltage oscillation in the line to which the sources are connected, and protection issues are some of these problems.

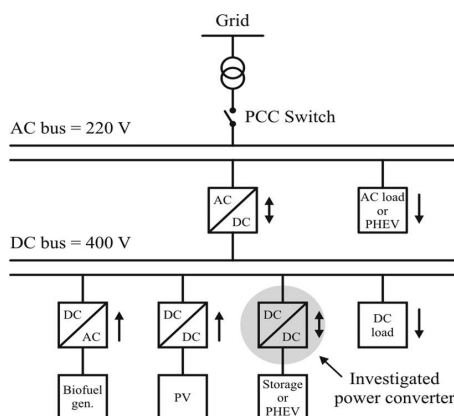


Fig.1 Residential micro grid system under study.

As an alternative to reduce such problems, the micro grid concept has been gaining more notoriety each day [5], [6]. Some ad-vantages of the micro grids are the possibility to generate electric power with lower environmental impact and easier connection of these sources to the utility, including the power management capability among their elements. This



International Journal of Advanced Research in Electrical, Electronics and Instrumentation Engineering

(An ISO 3297: 2007 Certified Organization)

Vol. 5, Issue 5, May 2016

configuration results in high efficiency, high reliability, and no frequency or phase control requirements, when compared to the ac inter connection bus [7], [8]. Moreover, it has low distribution and transmission losses, low cost, the possibility to operate across long distances, and it does not use transformers, in turn leading to volume and cost reduction [2]. Considering the local generation of distributed sources, residential micro grids are being proposed as an interesting solution for increasing renewable energy production and system reliability for household appliances. The residential micro grid under study here, as shown in Fig. 1 [9], Comprises two DG sources (photovoltaic panels and bio fuel generator), an energy storage system (one battery and one super capacitor bank), and a plug-in hybrid electric vehicle (PHEV). Moreover, it is able to supply both ac and dc loads. The micro grid has two buses: one main dc bus in which the DG sources, storage devices, and dc loads are connected, and one ac bus in which the ac loads are connected and the point of common coupling (PCC) with the utility grid is located. The arrows beside each converter indicate the possible power flow directions. The investigated power converter in this paper is also indicated. Table I presents the micro grid sources and converter power levels. Further information can be found in [9].

In the micro grid systems, the energy storage system is of great importance. It is responsible for supplying energy to the loads when the main sources are not capable during short periods of time and steady-state operation the proposed residential micro grid energy storage system composed of a battery bank and a super capacitor bank has two main functions. The battery bank acts as a backup device due to its high energy density [10], providing energy under the steady state condition when the other sources are not capable. The super capacitor bank acts as a quick discharge device due to its high power density [11], providing energy to the micro grid during transitory periods, mainly during the bio fuel generator start-up time. Consequently, due to the importance of the energy storage system, this paper focuses specifically on the dc power module of the micro grid energy storage system.

Table I
Micro grid Power Level

Element	Power(Kw)
Bio fuel generator	1.4
PV Panel	2.34
Battery bank	500
Super capacitor bank	1.4
Plug in hybrid	2.5
Power inverter	7.5
Residential Load	12

A dc–dc converter is necessary to connect the energy storage system to the micro grid dc bus. Once the super capacitor bank voltage is low and not controlled, the dc–dc converter must have a high voltage ratio between the input and output stages. More-over, it must be able to operate under a wide output power range. Since the super capacitor and battery banks are not demanded at the same time according to the micro grid operation, the same converter is used for both, including a selector switch to choose the appropriate storage device for each situation. Several dc–dc converter topologies employing a super capacitor bank to complement the energy supplied by other sources, such as fuel cells, batteries, or generators, have been proposed in the literature[12]–[15].These topologies are applied to hybrid vehicles, uninterruptable power supply (UPS) systems, buses in general and critical loads, among other applications.

The dual active bridge (DAB) or modified DAB converters are approached in [12]–[14]. Papers [12] and [13] propose modulation schemes different from the conventional phase-shift modulation. In [12], a new hybrid modulation technique to expand the converter power range is proposed, while paper [13] proposes an optimal modulation scheme that enables minimum conduction and copper losses for a DAB converter. In [14], an input stage composed of a ZSI converter is proposed, which guarantees the voltage boost during the super capacitor discharge, but increases the number of active switches. In [15], a DAB converter including unified soft-switching scheme (voltage clamp branch on the current-fed bridge) is proposed. Paper [16] discusses the steady-state operation of a phase-shift modulated dual-bridge series resonant converter. In [17], design issues of the DAB converter such as leakage inductance, switching frequency, and turns ratio are approached aiming for higher efficiency. Paper [18] describes the design and performance of the converter and analyzes the effect of unavoidable dc-bias currents on the magnetic-flux saturation of the transformer. These topologies present high number of active devices and most of them present high input and output current ripple.

Topology presented in [18] has a particular configuration, in which the super capacitor bank is situated between two dc–dc converters that connect another energy source to the load. Paper [19] applies a full-bridge with active clamping and a half-bridge converter, but uses batteries and fuel cells. A common feature of these topologies is that a transformer is used to aid voltage boosting due to the low voltage level of the super capacitor bank, besides providing galvanic isolation. The exception is a no isolated converter presented in [20]. However, in this case the super capacitor bank voltage level is much higher than in the other topologies. Consequently, the desired converter must present the following features: bidirectional power flow, high power operation, galvanic isolation, high usage of the super capacitor stored energy, and long battery lifetime. High usage of the super capacitor stored energy is achieved through a deeper discharge, making it reach lower voltage levels (requiring high voltage ratio). A long battery lifetime is achieved by draining from and providing to the battery a low ripple dc current.

The DAB converter, shown in Fig. 2, which is the most used topology for this application, is formed by two full-bridge converters connected through a transformer. It needs an elevated number of active devices thereby resulting in high cost. It also presents a high input and output current ripple, the soft switching only occurs on a specific operation range, and the phase shift ϕ between the two modules should not be higher than 50° in order to limit the circulating reactive power [19]. This converter is appropriate for situations in which both charging and discharging processes demand high power levels [12], which is not the case regarding the desired application, as presented hereinafter.

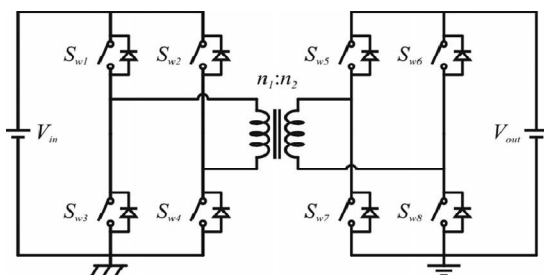


Fig. 2. DAB converter

A dc–dc bidirectional converter can be added between the energy storage device and one of the full-bridges [20], as shown in Fig. 3. It provides advantages, such as to extend the battery lifetime by maintaining the supplied current with a low ripple, to obtain better usage of the super capacitor stored energy (over 85%) by lowering the super capacitor voltage level, and to reduce the full-bridge switches current level and cost by boosting the voltage from the energy storage system to an intermediate value. Fig. 4 shows a comparison of the storage system current for both converters rated at 1.4 kW, where a considerable reduction on the current ripple can be seen when the bidirectional converter is included, which leads to a longer lifetime for the storage system. A complete comparison considering several parameters among these converters and the converter proposed in this paper is shown in Section IV.

This paper is organized as follows. Section II presents the proposed integrated full-bridge-forward converter. Three clamping circuits are studied and applied to the proposed converter. Section III presents the transformer design methodology. A comparison between the proposed converter and the DAB converter is performed in Section IV. The experimental results are included in Section V as well as an efficiency comparison among the Clamping circuits applied to the proposed converter. Section VI presents the main conclusions of this paper.

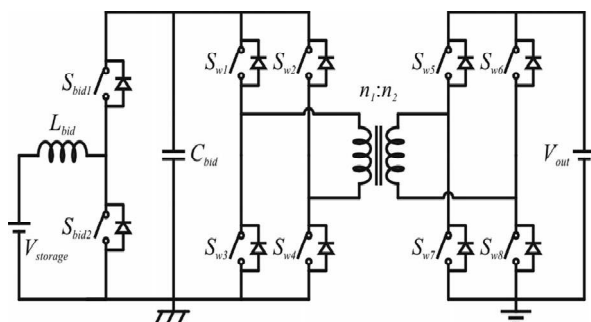


Fig. 3. DAB including a bidirectional converter

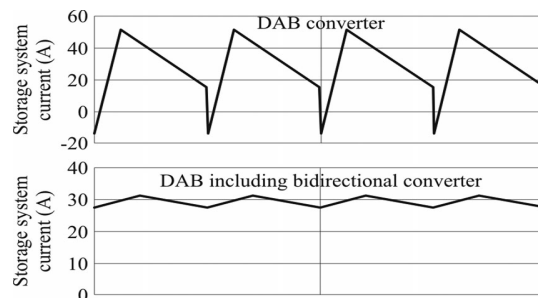


Fig. 4. Storage system current comparison ($V_{in} = 48V$, $V_{out} =$

II. PROPOSED INTEGRATED FULL-BRIDGE FORWARD DC-DC CONVERTER

The proposed converter must be designed for both charging and discharging processes. The maximum designed power for the micro grid energy storage system discharging process is equal to 1.4 kW (high power during transitories), which is supplied by the super capacitor bank. The isolated static power converter traditionally used in applications with this power level (above 1 kW) is the full-bridge converter, shown in Fig. 5.

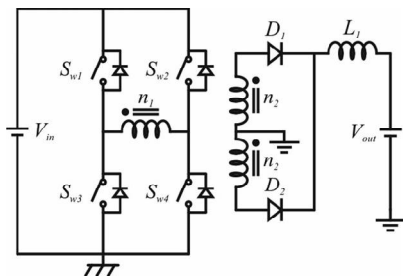


Fig. 5. Full-bridge converter.

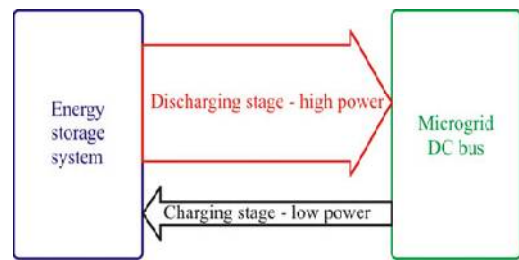


Fig. 6. Power level transfer diagram for the application.

The charging process of the micro grid energy storage system does not need to be performed with the same power level of the discharging process. Once the energy storage system of a residential micro grid is not often demanded due to the low electric energy supply interruption indices, there is a long period of time available between two interactions. This way, the charging process can have a longer duration and, consequently, be performed with lower power levels (100 W, for example). To illustrate, Fig. 6 shows a diagram with the relative power levels for the application. Therefore, it is not necessary to use another full-bridge converter for the charging process. Due to the presence of the full-bridge converter for the discharging process, it is possible to utilize the respective active switches to rectify the converter output voltage during the charging process. This way, it is necessary to add only the input stage of the respective converter for the charging process. One of the simplest converters for this application is the forward converter, as shown in Fig. 7, which demands only one active switch and is appropriate for the related power levels.

Therefore, the proposed dc-dc converter, shown in Fig.8, is the integration of a full-bridge and a forward converter. The Full-bridge converter is responsible for the energy storage system discharging stage, while the forward converter is responsible for the energy storage system charging stage. Moreover, other advantages are that it provides the use of a transformer turns ratio (tertiary higher than secondary) that avoids the circulation of reactive energy during the charging process, which will be further discussed in Section III, and the storage system voltage can be reduced without penalizing the full-bridge converter operation, once its input voltage is kept constant. During the energy storage system discharging stage, the bidirectional converter boosts the voltage from the energy storage system to an intermediate level, while during the energy storage system charging stage; it performs voltage post regulation or remains with S_{bid1} ON and S_{bid2} OFF acting as a low-pass filter, thus eliminating the switching losses. The second option is chosen in this paper, where only the conduction losses are present, which are of very low value due to the low power stage. Since the bidirectional converter can be added at the input of several converters, including the proposed one, the DAB converter and any converter where a low ripple input current is important, but its insertion is not necessary, The following detailed analysis about the insertion of this converter is presented in Section III.

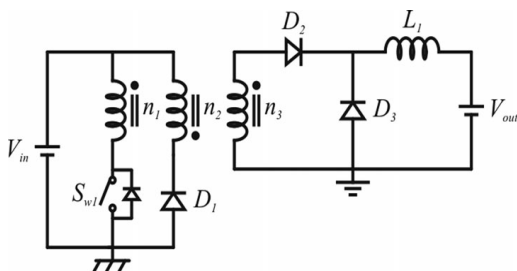


Fig.7. Forward converter

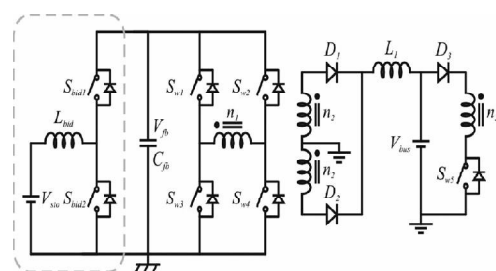


Fig.8. Proposed integrated full-bridge-forward dc-dc converter including bidirectional converter.



International Journal of Advanced Research in Electrical, Electronics and Instrumentation Engineering

(An ISO 3297: 2007 Certified Organization)

Vol. 5, Issue 5, May 2016

Taking into account the full-bridge-forward topology with-out the bidirectional converter, it presents a reduced part count compared to the full-bridge and forward topologies without the integration process achieved due to the elimination of one Transformer, two diodes, and one inductor, resulting in a lower implementation cost. The integration process and the bidirectional power flow characteristic provide for the use of only one converter to connect the energy storage system to the dc bus, simplifying the dc bus voltage regulation and micro grid management process. The proposed topology has a simple energy storage system charging process compared to the DAB converter, once it requires only one active switch and drive circuit compared to four in its counterpart.

The energy storage system discharging stage is identical to the traditional full-bridge converter operation. The charging stage, on the other hand, presents some differences compared to the traditional forward converter operation, namely, the output stage of the converter has a full-bridge characteristic instead of a freewheeling stage constituting a double-ended forward converter; the transformer demagnetizing process is executed by the anti-parallel diodes of the full-bridge converter switches and a clamping circuit (shown ahead), instead of one additional transformer winding; and the output inductor is eliminated. A three-winding transformer is required in this topology. Windings 1 and 2 are used in the full-bridge operation, and windings 1 and 3 in the forward operation. One diode needs to be added in series with the transformer tertiary winding to avoid current circulation through the anti-parallel diode of the forward converter switch during full-bridge converter operation mode.

A. Proposed Converter Including Dissipative Passive Clamping Circuit

In order to avoid voltage spikes during the turn-off of the forward converter active switch due to the interruption of the current through the transformer leakage inductance, one passive clamping circuit is first added in parallel to this switch. This clamping circuit is composed of one diode, one capacitor, and one resistor, as shown in Fig. 9. Moreover, this circuit plays a role in the transformer demagnetizing process, once the clamping voltage is applied on the transformer tertiary winding during two operation subintervals and a certain amount of current circulates through it.

The energy storage system discharging process is identical to the traditional full-bridge converter [29], as aforementioned; thus, it will not be analyzed in detail, but experimental results are provided in Section V. Special attention is focused on the energy storage system charging process (double-ended forward converter) due to its particularities. This process is divided into five subintervals for the converter operating in the discontinuous conduction mode illustrated in Fig. 10. All semiconductor switches are considered ideal and the resistor and capacitor of the passive clamping circuit are replaced by an ideal dc source for the analysis. The variable n stands for n_3/n_1 .

First Stage: This stage, shown in Fig. 10(a), starts when the forward converter switch S_{w5} is turned ON. The anti-parallel diodes of the S_{w1} and S_{w4} switches also turn ON once they are forward biased. Positive voltages are applied to the transformer magnetizing (1) and primary (2) and tertiary (3) leakage inductances. Therefore, the currents through these elements increase.

$$V_{Lm} - 1(t) = \frac{L_m (n2Ld1V_{bus} + nV_{fb}Ld3)}{n2Ld1(L_m + Ld3) + L_mLd3} \quad (1)$$

$$V_{Ld} - 1(t) = \frac{V_{Lm} - 1(t)}{n} - V_{fb} \quad (2)$$

$$V_{Ld3-1}(t) = V_{bus} - V_{Lm} - 1(t) \quad (3)$$

Second Stage: This stage, shown in Fig. 10(b), starts when the forward converter switch turns OFF. Therefore, the clamping diode D_{cl} turns ON, assuming the current that circulated through the forward converter switch. This current decreases because a negative voltage (4) is applied to the tertiary winding leakage inductance. The currents through the anti parallel diodes of the S_{w1} and S_{w4} switches also decrease because the voltage applied to the primary winding leakage inductance (5) becomes negative. In this subinterval, the magnetizing current is deviated to the clamping circuit, resulting in losses for the topology. The clamping circuit voltage causes overvoltage on the forward converter switch; however, a high value reduces the duration of this and the next stages, reducing the clamping circuit losses. The voltage across the magnetizing inductance is given by (6),

Third Stage: This stage, shown in Fig. 10(c), starts when the anti-parallel diodes of the S_{w1} and S_{w4} switches turn OFF, since the current through them reaches zero, and the anti-parallel diodes of the S_{w2} and S_{w3} switches turn ON. The current through these diodes increases because the voltage applied to the primary winding leakage inductance (7) continues negative. Therefore, the current through the primary winding is inverted. The current through the clamping circuit diode continues to decrease once the voltage applied to the tertiary winding leakage inductance (8) keeps negative, but with a lower rate. Therefore, in this subinterval, the magnetizing current is gradually transferred from the clamping circuit to the converter output. The voltage across the magnetizing inductance is given by (9)

International Journal of Advanced Research in Electrical, Electronics and Instrumentation Engineering

(An ISO 3297: 2007 Certified Organization)

Vol. 5, Issue 5, May 2016

$$V_{Ld3} - 2(\delta) = V_{bus} - V_{cl} - V_{Lm} - 2(\delta) \quad (4)$$

$$V_{Ld1} - 2(\delta) = \frac{V_{Lm} - 2(\delta)}{n} - V_{th} \quad (5)$$

$$V_{Lm} - 2(\delta) = \frac{I_m (n^2 L_{d1} (V_{bus} - V_{cl}) + n V_{th} L_{d3})}{n^2 L_{d1} (L_m + L_{d3}) + L_m L_{d3}} \quad (6)$$

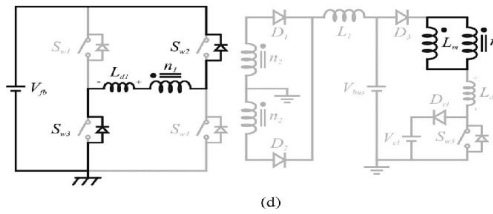
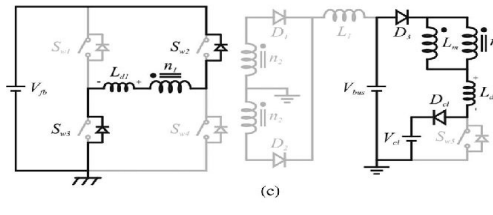
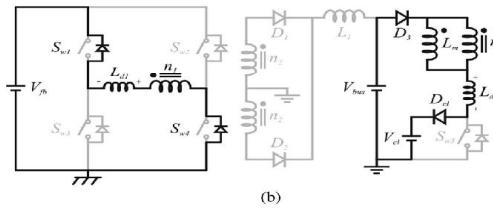
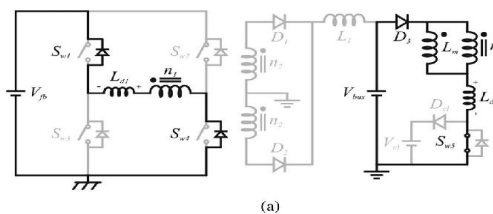
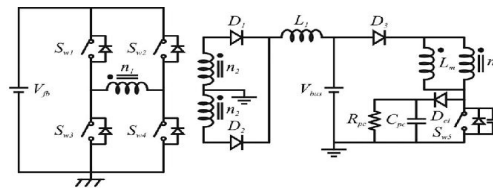


Fig.10: Operation stages of the proposed converter with passive clamping : (a) First stage, (b) Second stage, (c) Third stage, and (d) fourth stage.

Fourth Stage: This stage, shown in Fig. 10(d), starts when the current through the clamping circuit diode D_{cl} reaches zero and it turns OFF. The currents through the anti parallel diodes of The S_{w2} and S_{w3} switches decrease once the voltage applied to the primary winding leakage inductance (10) becomes positive. The voltage applied to the tertiary winding leakage inductance (11) is equal to zero and applied to the magnetizing inductance is given by (12).

$$V_{Ld1} - 3(\delta) = \frac{V_{Lm} - 3(\delta)}{n} - V_{th} \quad (7)$$

International Journal of Advanced Research in Electrical, Electronics and Instrumentation Engineering

(An ISO 3297: 2007 Certified Organization)

Vol. 5, Issue 5, May 2016

$$v_{Ld3} - 3(t) = V_{bus} - v_{cl} - v_{Lm} - 3(t) \quad (8)$$

$$v_{Lm} - 3(t) = \frac{L_m (n^2 L_{d1} (V_{bus} - v_{cl}) + nV_{fb}L_{d3})}{n^2 L_{d1} (L_m + L_{d3}) + L_m L_{d3}} \quad (9)$$

Fifth Stage: This stage starts when the anti-parallel diodes of the S_{w2} and S_{w3} switches turn OFF once the current through them reaches zero. The voltages applied to the primary and tertiary windings leakage inductances, and converter current are equal to zero. This stage ends when the forward converter switch S_{w5} is turned ON, starting the next operation period. Fig. 11 shows the main waveforms of the converter operating in discontinuous conduction mode. These waveforms are forward converter switch current $i_{S_{w5}}$, clamping circuit diode current $i_{D_{cl}}$, magnetizing inductance current i_{L_m} , output current i_{fb} , voltages across the magnetizing inductance v_{L_m} , and primary $v_{L_{d1}}$ and tertiary $v_{L_{d3}}$ winding leakage inductances. The respective subintervals are also indicated.

$$v_{L_{d1}} - 4(t) = \frac{n^2 L_{d1} V_{fb}}{n^2 L_{d1} + L_m} \quad (10)$$

$$v_{L_{d3}} - 4(t) = 0 \quad (11)$$

$$v_{L_m} - 4(t) = \frac{nL_m V_{fb}}{n^2 L_{d1} + L_m} \quad (12)$$

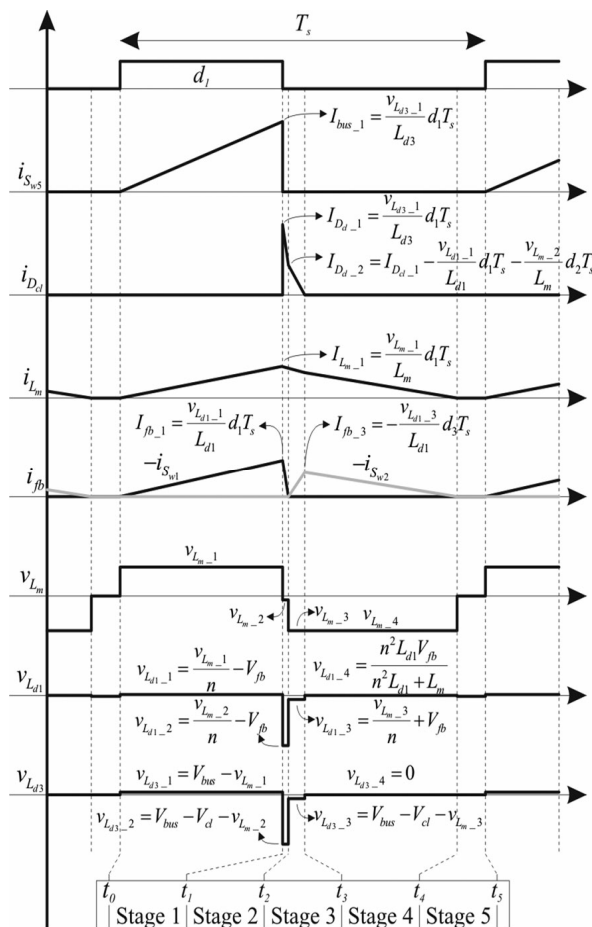


Fig 11. Main waveforms of the proposed converter with passive clamping parameters

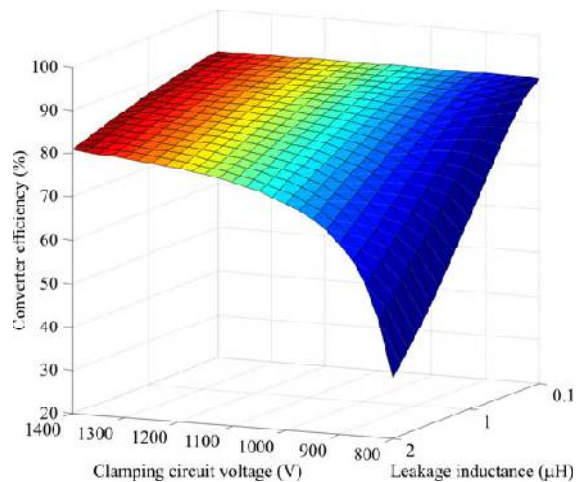
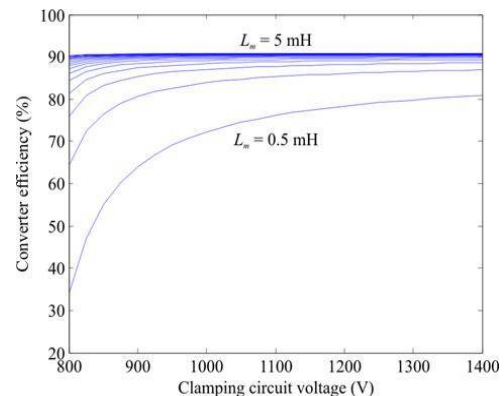


Fig.12. Converter efficiency depending on topology Parameters ($V_{bus} = 400V$, $V_{fb} = 52V$, $P_o = 100W$, $n_3:n_1 = 7:1$, $L_m = 2mH$).



Circuit. Fig.13. Converter efficiency depending on topology

($V_{bus} = 400V$, $V_{fb} = 52V$, $P_{out} = 100W$, $n_3:n_1 = 7:1$, $L_{d1} = 0.5\mu H$).

This topology solves the voltage spike problem. However, during the clamping circuit on state, the

magnetizing inductance current is deviated toward the passive elements. Based on equations deduced from the converter operation stages, several graphics can be obtained to analyze the converter efficiency depending on the converter parameters. Fig. 12 shows the graphic of the converter efficiency for distinct clamping circuit voltages and transformer primary winding leakage inductances. Fig. 13 shows the converter efficiency as a function of the clamping circuit voltage for different transformer magnetizing inductance values, varying from 0.5 to 5mH, with 0.5mH steps. The converter efficiency presented in these graphics is obtained considering only the losses dissipated in the clamping circuit a detailed analysis shows that the power losses can be reduced as the clamping circuit voltage and the transformer magnetizing inductance become higher, as well as the transformer leakage Inductance becomes lower. This occurs because the inversion of the current through the transformer primary winding occurs more quickly, reducing the amount of energy deviated toward the passive clamping circuit. Another way to improve the efficiency of the double-ended forward converter is using different types of clamping circuits. Two new topologies are proposed: a regenerative passive clamping circuit, presented in Section II-B, and a regenerative active clamping circuit, shown in Section II-C.

B. Proposed Converter Including Regenerative Passive Clamping

Using the same components of the dissipative passive clamping circuit shown in Fig. 9 and changing one of the resistor connection points, as shown in Fig. 14, it is possible to modify the clamping circuit in such a way that part of the deviated energy is regenerated back to the micro grid dc bus and a smaller part is dissipated over the resistor. One terminal of the resistor continues to be connected between the capacitor and diode of the clamping circuit, while the other terminal is connected between the dc bus and the diode in series with the transformer tertiary winding.

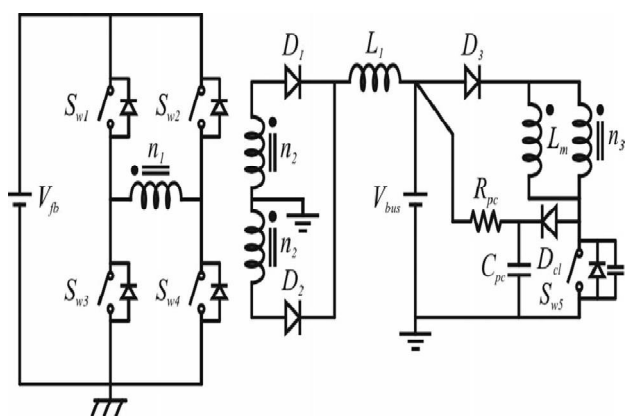


Fig.14. Proposed converter with regenerative passive clamping circuit.

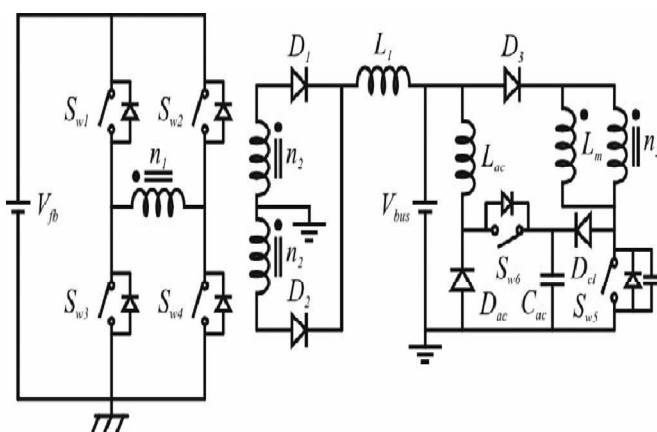


Fig. 15. Proposed converter with regenerative active clamping

Compared to the converter topology with dissipative passive clamping, for the same resistor value, the voltage across the clamping capacitor in this new topology increases, but the average voltage across the resistor is lower, as shown in Fig. 16(a), resulting in lower losses, as shown in Fig. 16(b). These results are obtained through converter simulation. The voltage across the resistor is given by the difference between the clamping capacitor voltage and the dc bus voltage. The operation stages are very similar compared to the previous clamping circuit and are not presented. The only differences are the voltage levels across the clamping capacitor and resistor, and consequently, the duration of the stages is slightly different.

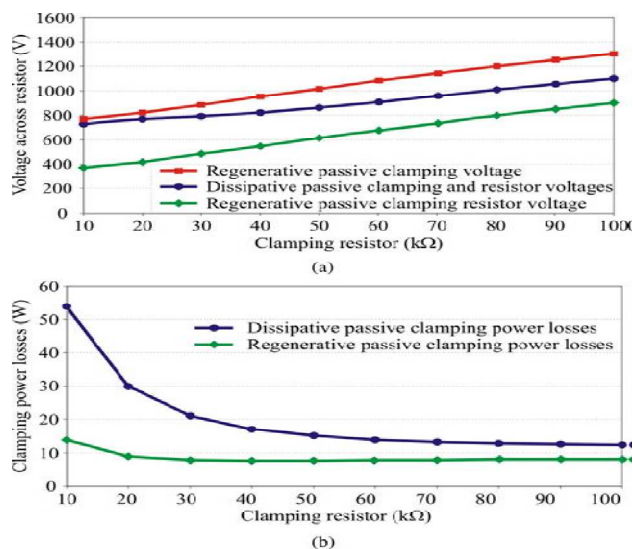
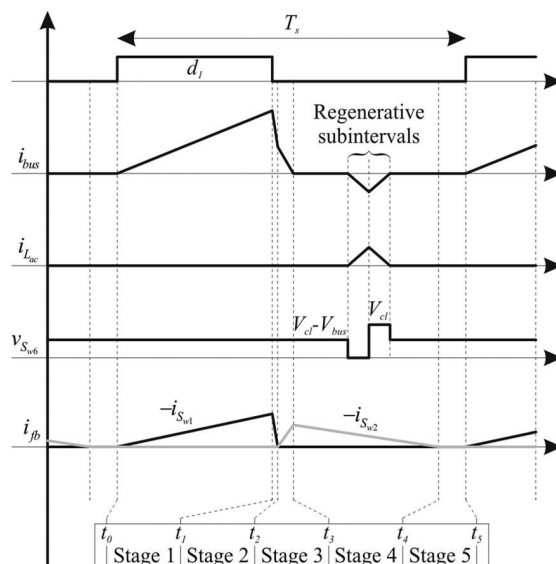


Fig.16. Clamping circuits' comparison:

Fig. 17. Proposed converter with active clamping waveforms
(a) Voltage across resistor and (b) Clamping power losses
($L_m = 2mH$).



($V_{bus} = 400\text{ V}$, $V_{fb} = 52\text{ V}$, $P_{out} = 100\text{ W}$, $n_3:n_1 = 7:1$, $L_{d1} = 0.5\mu H$,

C. Proposed Converter Including Regenerative Active Clamping

One alternative for reducing the losses over the clamping circuit even more is to use a regenerative active clamping circuit. For the double-ended forward topology under study special attention should be taken, since the active clamping circuit cannot regenerate energy to the micro grid dc bus through the transformer tertiary winding due to the presence of the series diode, thus eliminating the possibility of use of some traditional active Clamping circuits. Considering this fact, the proposed forward converter with an active clamping topology is shown in Fig. 15. Basically, the clamping resistor is replaced by an active switch, a diode, and an inductor. The energy stored in the clamping capacitor due to the current i_{Dcl} , shown in Fig. 11, is delivered back to the dc bus, instead of being dissipated over a resistor. The active clamping circuit switch can be turned ON during any forward converter operation stage. The switch on time (duty cycle) is an important factor to determine the voltage level across the clamping circuit. The lower the switch on time, the higher the clamping circuit voltage and, consequently, a lower portion of energy is deviated toward the clamping circuit, reducing the switching and conduction losses on this circuit, and increasing the converter efficiency. This feature is presented in Section V. In this converter, there are two additional operation stages. One in which the clamping circuit current circulates through S_{w6} and L_{ac} , and another in which the current circulates through D_{ac} and L_{ac} . Fig. 17 shows the main waveforms of the converter with an active clamping circuit operating in discontinuous conduction mode. These waveforms are dc bus current i_{bus} , clamping circuit inductor current i_{Lac} , voltage across the clamping circuit switch V_{Sw6} , and output current i_{fb} . An efficiency comparison among the three different clamping circuits applied to the double-ended forward converter is shown in Section V

TABLE II
CONVERTER PARAMETERS

Parameter	Symbol	Value
DC Bus voltage	V_{Bus}	400V
Full bridge charging voltage	V_{charg}	50 TO 55V
Full bridge discharge voltage	V_{fb}	80V
Nominal storage system voltage	V_{sto}	48V
Minimum storage system voltage	$V_{sto-min}$	24V
Maximum forward switch voltage	$V_{sw5-max}$	1200V
Nominal charging power	P_{ch}	100V
Maximum discharging power	P_{disch}	1.4kW



International Journal of Advanced Research in Electrical, Electronics and Instrumentation Engineering

(An ISO 3297: 2007 Certified Organization)

Vol. 5, Issue 5, May 2016

III. TRANSFORMER DESIGN METHODOLOGY

This section presents a design methodology for the transformer of the proposed full-bridge-forward integrated converter including a bidirectional converter, as shown in Fig. 8, based on the parameters shown in Table II.

The turns ratio n_2/n_1 between the primary and secondary transformer windings must be such that it allows the voltage boost from the bidirectional converter of the energy storage System voltage level V_{fb} to the dc bus voltage level V_{bus} , so that

$$\frac{n_2}{n_1} > \frac{V_{bus}}{V_{fb} \cdot D_{ef}} \quad (13)$$

Where D_{ef} is the effective full-bridge converter duty cycle. For the adopted converter parameters and assuming D_{ef} equal to 0.85, this relation must be higher than 5.5. On the other hand, the turns ratio n_3/n_1 between the tertiary and primary transformer windings must be lower than the relation between V_{bus} and V_{charg} in order to allow the storage system charging process, then

$$\frac{n_3}{n_1} > \frac{V_{bus}}{V_{charg}} \quad (14)$$

For the adopted converter parameters, this relation must be lower than 8; otherwise, the voltage across the energy storage system does not reach 50 V needed for the charging process. In addition, the turns ratio n_3/n_1 between the tertiary and primary transformer windings must also be such that the sum between the reflected tertiary voltage on full-bridge converter operation and the dc bus voltage is lower than the maximum forward converter switch breakdown voltage $V_{Sw5 \max}$, once this voltage is applied across the clamping circuit capacitor. Therefore, this turns ratio must respect (15) and, for the adopted converter parameters, it must be lower than 8.42

$$\frac{n_3}{n_1} > \frac{V_{Sw5 \max} - V_{bus}}{V_{fb}} \quad (15)$$

The turns ratio n_3/n_2 between the tertiary and secondary transformer windings must respect (16) to prevent current circulation through the diodes of the secondary bridge during the forward converter operation stages in which a negative voltage is applied across the tertiary winding

$$\frac{n_3}{n_1} > \frac{V_{fb} - V_{bus}}{V_{bus}} \quad (16)$$

If this ratio is lower than 1, the upper diode D_1 starts to conduct ($n_2 - D_1 - L_1 - V_{bus}$) and if (16) is not satisfied, the bottom diode D_2 starts to conduct ($n_2 - D_2 - L_1 - V_{bus}$), resulting in additional power losses, but which are very low due to the small current value. For the adopted converter parameters, this relation must be higher than 1.25.

Taking into account that the proposed converter must operate under the residential micro grid power, voltage, and current parameters, which are shown in Table II, to achieve proper operation, the transformer turns ratio must follow the relation

$$1 < \frac{n_2}{n_1} < \frac{n_3}{n_1} < 8 \quad (18)$$

The transformer has great importance in the converter performance, as it influences the converter efficiency not only due to its inherent losses, but also due to the clamping circuit losses depending on the magnetizing and leakage inductances. Therefore, careful attention should be paid to its design. Taking into account the presented design methodology, the chosen transformer turns ratio is $n_1 = 1$, $n_2/n_1 = 6$, and $n_3/n_1 = 7$.

The presence of the bidirectional converter is recommended when a high efficiency performance is desired, but is not necessary on the proposed topology when a low final cost is important. If the bidirectional converter is not applied, (17) cannot be respected, since the turns-ratio n_2/n_1 needs to be higher than n_3/n_1 , in order to provide voltage boost from the energy storage system to the dc bus and voltage reduction from the dc bus to the energy storage system. However, in this case the transformer secondary winding conducts ($n_2 - D_1 - L_1 - V_{bus}$) during the forward converter operation stage. This improper conduction leads to power losses and lowers the converter efficiency, but does not make proper converter operation impracticable. The inclusion of the bidirectional converter solves this efficiency problem, but mainly brings several advantages to the topology, equal to the ones discussed for the DAB converter.



International Journal of Advanced Research in Electrical, Electronics and Instrumentation Engineering

(An ISO 3297: 2007 Certified Organization)

Vol. 5, Issue 5, May 2016

IV. COMPARISON BETWEEN DAB AND PROPOSED CONVERTER

The main objective of this section is to compare the pro-posed topology with the most used and consolidated converter for similar applications, which is the DAB converter. The DAB converter, DAB including a bidirectional converter and the pro-posed converter including a bidirectional converter are com-pared in Table III in terms of number of devices, current levels at the input, output, transformer, and active switches of the converters operating at nominal power.

In order to make a fair comparison, the transformer turns ratio $n_1:n_2$ and operation frequency have been chosen to be the same. Moreover, the parameter known as d , given by (18), has been kept near to 1 for the three converters.

TABLE III
CONVERTERS COMPARISON

Parameters	DAB	DAB Bidirectional	FB Forward bidirectional
Active switches	8	10	7 or 8 with active clamping
Inductors	0	1	2
Diodes	0	0	4
RMS input (storage)Current(A)	32.71	29.53	29.31
Input current ripple(A)	62.89	3.96	3.82
RMS output DC bus current(A)	5.45	3.96	3.5
Output current ripple(A)	16.61	7.40	0.45
RMS Primary current(A)	32.71	23.73	22.01
RMS Secondary current(A)	5.45	3.96	3.45
Transformer current ratio	1:6	1:6	1:6:7
Transformer core volume(cm ³)	78.21	78.21	78.20
Transformer leakage inductance(μH)	4	6.67	1
Phase shift angle(degrees)	41	41	161
Bidirectional converter RMS Switch current (A)	-	22.85	22.69
Primary full bridge RMS Switch current(A)	23.58	16.79	18.67
Secondary full bridge RMS Switch current(A)	3.91	2.80	-
Primary full bridge RMS Switch voltage (V)	48	80	80
Secondary full bridge RMS Switch voltage (V)	400	400	-

This brings advantages mainly for the DAB converter operation, since it guarantees a wider power range with ZVS and lower ripple levels for the currents through the converter input, output, transformer, and active switches. The transformer leakage inductance had to be increased for both DAB converters to adjust the input and output voltage levels, maintaining d near to 1. Values from Table III have been obtained employing conventional phase-shift modulation for the DAB converters at nominal power, since it is easy to implement, allows ZVS operation, has higher power transfer capability compared to triangular and trapezoidal modulations, and provides lower RMS current both in transformer and the switches and causes a lower peak current compared to the aforementioned modulation schemes [12].

$$d = \frac{n1.Vout}{n2.Vin} \quad (18)$$

The transformer volume is practically the same for the three converters. The core volume is the same. The copper volume is almost the same because the turns ratio is equal, but the current levels through DAB and DAB with a bidirectional converter are higher than in the proposed converter, demanding more parallel wires, while the proposed converter demands an additional tertiary winding designed for small charging current. The proposed converter presents lesser number of active de-vices than the DAB converters, but more passive devices. However, it is important to highlight that the two Inductors provide considerably low input and output currents ripple, one of the main objectives for the application. The DAB converter, on the other hand, presents very high input and output current ripple. The DAB

International Journal of Advanced Research in Electrical, Electronics and Instrumentation Engineering

(An ISO 3297: 2007 Certified Organization)

Vol. 5, Issue 5, May 2016

with a bidirectional converter presents high output current ripple and demands ten semiconductor switches. Regarding the proposed converter, the RMS input, output, and transformer currents are similar, but lower than its counterparts, demanding less parallel wires. The RMS switches' currents are also similar, demanding practically the same devices' current levels. Therefore, it can be concluded that low input and output current ripples are achieved with less or the same number of active devices, without compromising the transformer volume and the switches current levels.

V. EXPERIMENTAL RESULTS

This section presents some experimental results of the full bridge converter, which is responsible for the energy storage system discharging process and of the double-ended forward converter without an output inductor originated from the proposed integration process, which is responsible for the energy storage system charging process. The bidirectional converter is not inserted. The three studied forward converter clamping circuits are approached. The converter parameters are presented in Tables II and IV.

TABLE IV
TOPOLOGY PARAMETERS

Parameters	Symbol	Value
Transformer turns ratio	$n1:n2:n3$	1:6:7
Switching frequency	f_s	50kHz
Clamping circuit capacitor	C_{pc}, C_{ac}	13nF
Output capacitor	C_{fb}	100 μ F
Active clamping circuit inductor	L_{ac}	5.4mH
Full bridge Converter output inductor	L_1	1350 μ H

A. Full-Bridge Converter

Experimental waveforms of the full-bridge converter applying phase-shift modulation are shown in Fig. 18. The current through the output inductor and transformer primary winding, and the voltage across the transformer primary winding are presented, when the output power is equal to 1.4 kW (phase-shift angle equal to 166°). Fig. 19 presents the efficiency of the full bridge converter and the efficiency of the full-bridge converter when it is integrated to the forward converter, as proposed in this paper.

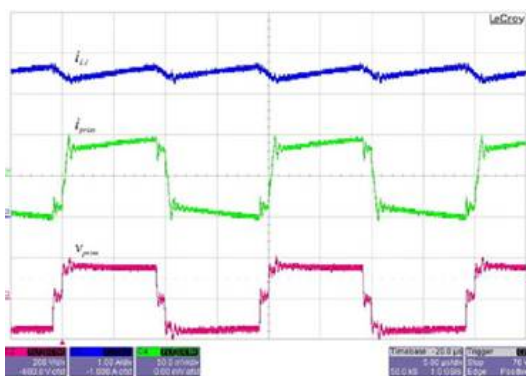


Fig.18. Current through the output inductor (1 A/div.), current through efficiencies

The Transformer primary winding (25 A/div.), and voltage across The transformer Primary winding (100 V/div.) ($V_{fb} = 80$ V, $V_{bus} = 400$ V, $P_{out} = 1.4$ kW, $n1:n2 = 1:6$).

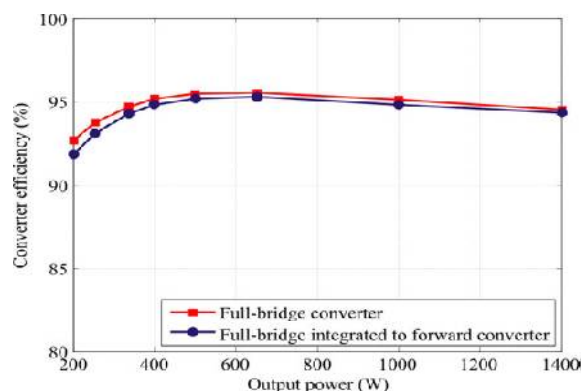


Fig.19. Full-bridge and full-bridge integrated to forward

($V_{fb} = 80$ V, $V_{bus} = 400$ V, $n1:n2 = 1:6$).

The efficiency of the capacitor charged. The efficiency difference reduces as the converter output power gets higher and is equal to 0.15% at 1.4 kW. This result proves that the impact of the proposed integration process full-bridge converter integrated to forward is slightly small due to the circulation of a low-value. Current through the forward converter ($V_{bus}-D3-n3-Dc1-C_{pc}$), which maintains the clamping over the full-bridge Converter efficiency, is not significant and that high efficiencies can be obtained.

B. Forward Converter with Dissipative Passive Clamping Circuit

The experimental results of the converter shown in Fig. 9, with the duty cycle of the forward switch equal to 0.25 in order to achieve the desired output voltage and power levels, are presented. Fig. 20 presents the transformer tertiary winding current and the forward converter switch voltage, respectively. It can be seen that the tertiary winding current is composed of the forward converter switch current and the clamping circuit diode current, both shown in Fig. 11. Fig. 21 shows the current and voltage across the transformer primary winding. It can be seen that the current is formed by $-i_{Sw1}$ and the opposite of $-i_{Sw2}$, both shown in Fig. 11, once the current is obtained in the transformer winding and not after the rectifying bridge. The curvature seen on the current Waveforms appears because there is not an output inductor on the topology. Its role is played by the transformer leakage inductance. Due to the low value of the leakage inductance, the circuit intrinsic resistances (transformer windings, active switch, diodes), which also have low values, constitute an LR circuit responsible for the current curvature. However, this curvature does not compromise the converter operation. The waveforms of the converter applying the regenerative passive clamping circuit shown in Fig. 14 are very similar to the waveforms of the converter applying the dissipative passive clamping technique and are not presented here. As aforementioned, the forward converter operation and efficiency has great dependence on the transformer magnetizing and leakage inductance values. Therefore, two different transformers with the same turns ratio, but with distinct features were used to obtain the next experimental results. Transformer 1 has a magnetizing inductance equal to 8.6mH and a leakage inductance referred to primary winding equal to 0.7 μ H, while transformer 2 has a magnetizing inductance equal to 1.7mH and a leakage inductance referred to primary winding equal to 0.85 μ H.

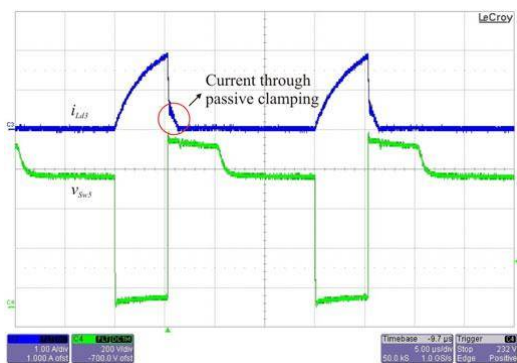


Fig. 20. Current on tertiary winding and forward converter switch voltage.

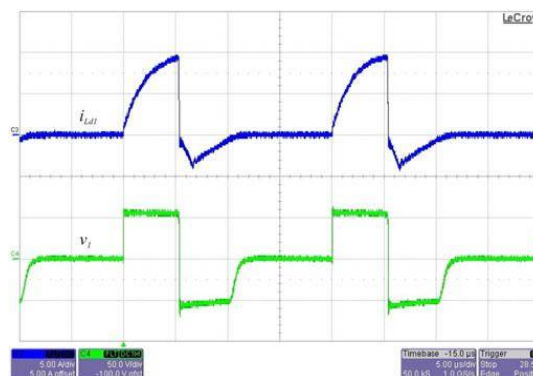


Fig. 21. Current and voltage on transformer primary winding.

Fig. 22 presents the converter efficiency for both transformers depending on the clamping circuit voltage, which is varied through the resistor of the clamping circuit. The output power is kept constant and equal to 100 W. It can be seen that the converter efficiency increases as the clamping circuit voltage increases for both Transformers, since less energy is deviated and dissipated over the clamping circuit, as expected by the theoretical analysis. It can also be seen that transformer 1 provides higher efficiency for the same clamping circuit voltage level. As aforementioned, the forward converter operation and efficiency has great dependence on the transformer magnetizing and leakage inductance values. Therefore, two different trans-formers with the same turns ratio, but with distinct features were used to obtain the next experimental results. Transformer 1 has a magnetizing inductance equal to 8.6mH and a leakage inductance referred to primary winding equal to 0.7 μ H, while transformer 2 has a magnetizing inductance equal to 1.7mH and a leakage inductance referred to primary winding equal to 0.85 μ H.

Fig.23 shows the converter efficiency with a wide output power range considering transformer 1. It can be seen that the converter efficiency increases as the output power increases, reaching higher efficiency at the nominal charging power.

C. Forward Converter with Regenerative Active Clamping Circuit

Experimental results for the converter with a regenerative active clamping circuit shown in Fig. 16 are presented in Fig. 24, where the transformer tertiary winding or dc bus current i_{bus} and the active clamping inductor current i_{Lac} can be seen. There is a 180° phase shift between the switches turn-on signals. The main switch duty cycle is equal to 0.25, while the duty cycle of the active clamping circuit switch is equal to 0.03. It can be seen that the

current through L_{ac} inductor is regenerated to the dc bus, validating the theoretical waveforms shown in Fig. 17.

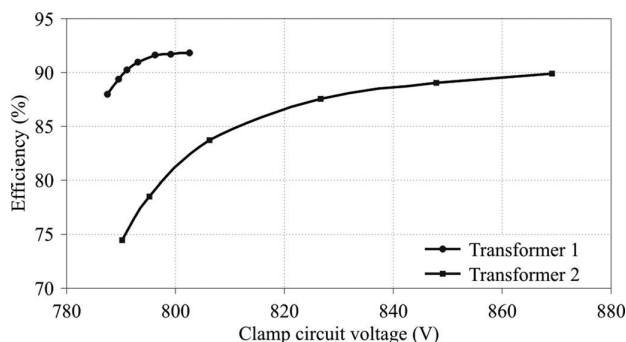


Fig. 22. Converter efficiency as a function of the clamping voltage for two variations
Distinct transformers ($V_{bus} = 400$ V, $V_{fb} = 54$ V, $P_{out} = 100$ W, $n_3 : n_1 = 7:1$ $n_3 : n_1 = 7:1$).

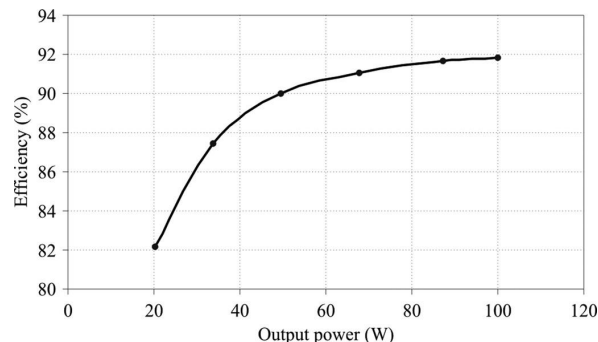


Fig.23. Converter efficiency with load variation using transformer 1 ($V_{bus} = 400$ V, $V_{fb} = 54$ V, $P_{out} = 100$ W, $n_3 : n_1 = 7:1$).

D. Efficiency Comparison among Forward Converter Clamping Circuits

Fig. 25 presents an efficiency comparison among the three clamping circuits applied to the double-ended forward converter. Transformer 1 has been used to obtain these results. The clamping circuit voltage is equal to 803 V for the three clamping circuits. It can be seen that the active clamping circuit presents higher efficiency, followed by the regenerative passive clamping circuit and, finally, by the dissipative passive clamping circuit. For the active clamping circuit, as the switch on time or the switching frequency decrease, the clamping circuit voltage increases and, consequently, a lower portion of current is deviated toward the clamping circuit. This way, the dc bus current falls to zero more rapidly when the main switch is turned OFF. With less energy flowing through the clamping circuit, the converter efficiency increases, as expected by the theoretical analysis. In order to obtain the same clamping circuit voltage as in the other clamping circuits, the active clamping switching frequency has been reduced to 10 kHz. Efficiency higher than 92% is achieved.

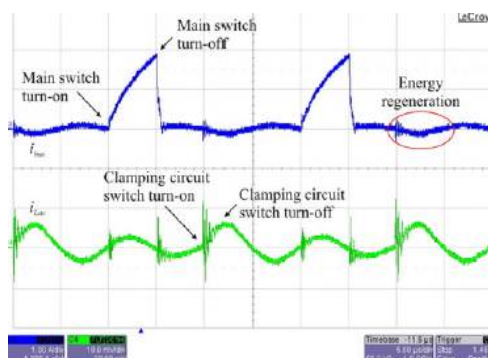


Fig.24. Currents through the dc bus (1 A/div.) and clamping circuit inductor (200mA/div.).
 $n_3 : n_1 = 7:1$

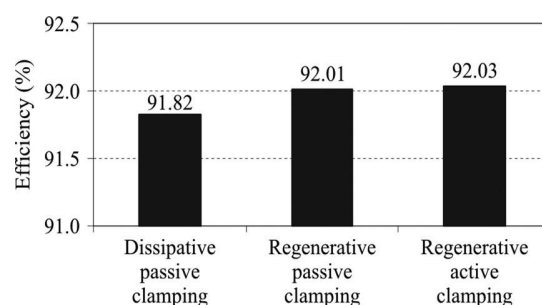


Fig.25. Converter efficiency applying three clamping circuits
($V_{bus} = 400$ V, $V_{fb} = 54$ V, $V_{cl} = 803$ V, $P_{out} = 100$ W, $n_3 : n_1 = 7:1$).

VI. CONCLUSION

This paper proposes an integrated full-bridge-forward dc-dc converter to connect the energy storage system to the dc bus of a residential microgrid. The converter major advantages are reduced active switches compared to the DAB



International Journal of Advanced Research in Electrical, Electronics and Instrumentation Engineering

(An ISO 3297: 2007 Certified Organization)

Vol. 5, Issue 5, May 2016

converter and individual topologies, high usage of the super capacitor bank stored energy, and a long battery bank lifetime. The proposed topology presents low input and output current ripple, high volt-age ratio, high power operation on the discharging process, galvanic isolation, and bidirectional power flow, as requested by the application.

Special attention is focused on the double-ended forward converter originated from the integration process. Three different clamping circuits (dissipative passive, regenerative passive and regenerative active) are studied, showing the converter operation stages, waveforms, and main features of each one. A transformer design methodology is also presented, where it is shown that the transformer has great importance on the converter performance once it influences the converter efficiency, which is basically due to the impact on the energy deviated through the clamping circuit. A comparison between the proposed converter and the DAB converter is made in terms of number of devices and current levels in several points of the topology, where it can be seen that the proposed converter presents low input and output current ripple, and demands lower number of active devices when passive clamping circuits are applied. An efficiency comparison shows that the proposed converter with regenerative active clamping circuit achieves higher efficiency. Efficiency over 92% is experimentally obtained.

REFERENCES

- [1] K. Sun, L. Zhang, Y. Xing, and J. M. Guerrero, "A distributed control strategy based on DC bus signalling for modular photovoltaic generation systems with battery energy storage," *IEEE Trans. Power Electron.*, vol. 26, no. 10, pp. 3032–3045, Oct. 2011.
- [2] F. A. Farret and M. G. Simoes, " *Integration of Alternative Sources of Energy*, 1st ed. New Jersey: Wiley, 2006.
- [3] Y. A.-R. I. Mohamed, "Mitigation of converter-grid resonance, grid-induced distortion, and parametric instabilities in converter-based distributed generation," *IEEE Trans. Power Electron.*, vol. 26, no. 3, pp. 983–996, Mar. 2011.
- [4] R. H. Lasseter and P. Paigi, "Microgrid: A conceptual solution," in *Proc. IEEE Power Electron. Spec. Conf.*, Jun. 2004, vol. 6, pp. 4285–4290.
- [5] H. Zhou, T. Bhattacharya, D. Tran, T. S. T. Siew, and A. M. Khambadkone, "Composite energy storage system involving battery and ultra capacitor with dynamic energy management in microgrid applications," *IEEE Trans. Power Electron.*, vol. 26, no. 3, pp. 923–930, Mar. 2011.
- [6] J.-Y. Kim, J.-H. Jeon, S.-K. Kim, C. Cho, J. H. Park, H.-M. Kim and K.-Y. Nam, "Cooperative control strategy of energy storage system and micro sources for stabilizing the microgrid during islanded operation," *IEEE Trans. Power Electron.*, vol. 25, no. 12, pp. 3037–3048, Dec. 2010.
- [7] R. S. Balog and P. T. Krein, "Bus selection in multi bus DC microgrids," *IEEE Trans. Power Electron.*, vol. 26, no. 3, pp. 860–867, Mar. 2011.
- [8] J. Chen, J. Chen, R. Chen, X. Zhang, and C. Gong, "Decoupling control of the non-grid-connected wind power system with the droop strategy based on a DC micro-grid," in *Proc. World Non-Grid-Connected Wind Power Energy Conf.*, 2009, pp. 1–6.
- [9] L. Roggia, C. Rech, L. Schuch, J. E. Baggio, H. L. Hey, and J. R. Pinheiro, "Design of a sustainable residential microgrid system including PHEV and energy storage device," in *Proc. Eur. Conf. Power Electron. Appl.*, 2011, pp. 1-9
- [10] F. Ongaro, S. Saggini, and P. Mattavelli, "Li-ion battery-super capacitor hybrid storage system for a long lifetime, photovoltaic-based wireless sensor network," *IEEE Trans. Power Electron.*, vol. 27, no. 9, pp. 3944–3952, Sep. 2012.
- [11] J. Cao and A. Emadi, "A new battery/ultra capacitor hybrid energy storage system for electric, hybrid, and plug-in hybrid electric vehicles," *IEEE Trans. Power Electron.*, vol. 27, no. 1, pp. 122–132, Jan. 2012.
- [12] H. Zhou and A. M. Khambadkone, "Hybrid modulation for dual-active-bridge bidirectional converter with extended power range for ultra capacitor application," *IEEE Trans. Ind. Appl.*, vol. 45, no. 4, pp. 1434–1442, Jul. 2009.
- [13] F. Krismer and J. W. Kolar, "Closed form solution for minimum conduction loss modulation of DAB converters," *IEEE Trans. Power Electron.*, vol. 27, no. 1, pp. 174–188, Jan. 2012.
- [14] D. Vinnikov, I. Roasto, and J. Zakis, "New bi-directional DC/DC converter for super capacitor interfacing in high-power applications," in *Proc. Int. Power Electron. Motion Control Conf.*, 2010, pp. T11-38–T11-43.
- [15] K. Wang, F. C. Lee, and J. Lai, "Operation principles of bi-directional full-bridge DC/DC converter with unified soft-switching scheme and soft-starting capability," in *Proc. IEEE Appl. Power Electron. Conf.*, 2000, vol. 1, pp. 111–118.
- [16] H. Tao, J. L. Duarte, and A. M. Hendrix, "Three-port triple-half-bridge bidirectional converter with zero-voltage switching," *IEEE Trans. Power Electron.*, vol. 23, no. 2, pp. 782–792, Mar. 2008.
- [17] M. Nowak, J. Hildebrandt, and P. Luniewski, "Converters with AC Transformer intermediate link Suitable as interfaces for super capacitor Energy Storage," in *Proc. IEEE Power Electron. Spec. Conf.*, Jun. 2004, vol. 5, pp. 4067–4073.
- [18] H. Tao, A. Kotsopoulos, J. L. Duarte, and M. A. M. Hendrix, "Multi Input bidirectional DC–DC converter Combining DC-link and magnetic Coupling for fuel cell Systems," in *Proc. IEEE Ind. Appl. Conf.*, Oct. 2005, vol. 3, pp. 2021–2028.
- [19] R. W. Erickson and D. Maksimovic, *Fundamentals of Power Electronics*. New York: Kluwer, 2004.
- [20] A. I. Pressman, *Switching Power Supply Design*. New York: McGraw-Hill, 1998.